A micromagnetic study of domain-structure modeling

Tetsuji Matsuo[a]*, Naoki Mimuro[a], Masaaki Shimasaki[b]

[a]Kyoto University, Kyoto 615-8510, Japan
[b]Fukui University of Technology, Fukui 910-8505, Japan

Abstract

To develop a mesoscopic model for magnetic-domain behavior, a domain structure model (DSM) was examined and compared with a micromagnetic simulation. The domain structure of this model is given by several domains with uniform magnetization vectors and domain walls. The directions of magnetization vectors and the locations of domain walls are determined so as to minimize the magnetic total energy of the magnetic material. The DSM was modified to improve its representation capability for domain behavior. The domain wall energy is multiplied by a vanishing factor to represent the disappearance of magnetic domain. The sequential quadratic programming procedure is divided into two steps to improve an energy minimization process. A comparison with micromagnetic simulation shows that the modified DSM improves the representation accuracy of the magnetization process.

1. Introduction

The micromagnetic simulation solving the LLG equation [1] is a powerful tool to describe the microscopic behavior of magnetic materials. However, it is difficult for the micromagnetic simulation to describe mesoscopic or macroscopic magnetic behavior because of its high computational cost. Several domain structure models (DSMs) [2]-[5] have been proposed to represent the mesoscopic behavior of magnetic materials. However, the capability of DSMs has not been sufficiently examined because they have not been compared with the micromagnetic simulation.

This paper modifies a DSM to improve its representation capability for the domain behavior. The modified DSM is compared with the micromagnetic simulation to examine its representation accuracy of the magnetization process.

2. Domain structure model

There are several DSMs [2]-[5] having different approaches for magnetostatic energy computation and magnetic energy minimization. This study examines Ref. [5]'s DSM.

The domain structure of all DSMs in Refs. [2]-[5] is given by several domains with uniform magnetization vectors and their boundaries (domain walls). Two-dimensional domain structures are studied in this paper. Fig. 1 illustrates an example of the domain structure where $\boldsymbol{m}_1, \ldots, \boldsymbol{m}_4$ are normalized magnetization vectors. The directions of magnetization vectors and the locations of domain walls are determined so as to minimize the total magnetic energy of the magnetic material.

The total magnetic energy E is given by

$$E = E_{\mathrm{ap}} + E_{\mathrm{an}} + E_{\mathrm{w}} + E_{\mathrm{st}} \tag{1}$$

where E_{ap} is the Zeeman energy, E_{an} is the anisotropic energy, E_{w} is the domain wall energy, and E_{st} is the magnetostatic energy.

The Zeeman energy is given as

$$E_{\mathrm{ap}} = -\mu_0 M d \sum_{i=1}^{N_{\mathrm{d}}} S_i \mathbf{m}_i \cdot \mathbf{H}_{\mathrm{ap}} \tag{2}$$
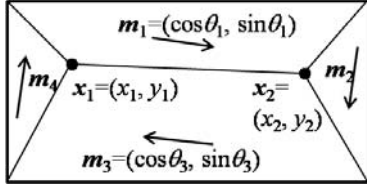
Fig. 1. Domain structure model.

where M is the magnitude of spontaneous magnetization, d is the thickness of the material, N_d is the number of assumed magnetic domains, S_i is the area of the i-th magnetic domain, and $\boldsymbol{H}_{ap}$ is the applied magnetic field.

The anisotropic energy is given as

$$E_{an} = K_1 d \sum_{i=1}^{N_d} S_i \sin^2 \theta_{ei} \qquad (3)$$

where a uniaxial anisotropy is assumed in this paper, K_1 is the anisotropy constant, and θ_{ej} is the angle between the easy-axis direction and the magnetization vector in the i-th domain.

The domain wall energy is given as

$$E_w = \sum_{j=1}^{N_w} E_{wj} \qquad (4)$$

where N_w is the number of domain walls and E_{wj} is the domain wall energy of the j-th domain wall. The Neel domain wall [1] is assumed in this study to analyze magnetic thin films. Accordingly, E_{wj} is given as

$$E_{wj} = 4L_j d \sqrt{A(K_1 + \frac{\mu_0 M^2}{2})} (1 - \cos\frac{\theta_{wj}}{2})^2 \qquad (5)$$

where A is the exchange stiffness constant, L_j is the length of the j-th domain wall, and θ_{wj} is the angle difference of adjacent magnetization vectors of the j-th domain wall.

The magnetostatic energy is determined from the magnetic charges on domain boundaries (domain walls and material boundaries). The magnetic charge density σ_j on the j-th domain wall is given as

$$\sigma_j = \mu_0 M (\boldsymbol{m}_{j1} - \boldsymbol{m}_{j2}) \cdot \boldsymbol{n}_j \qquad (6)$$

where $\boldsymbol{m}_{j1}$ and $\boldsymbol{m}_{j2}$ are adjacent normalized magnetization vectors of the j-th domain wall and $\boldsymbol{n}_j$ is the unit normal vector. For material boundaries, $\boldsymbol{m}_{j2} = 0$. The magnetic scalar potential φ is given as

$$\varphi = \sum_{j=1}^{N_b} \varphi_j = \frac{1}{4\pi\mu_0} \sum_{j=1}^{N_b} \int_{w_j} \frac{\sigma_j}{r} dS \qquad (7)$$

where N_b is the number of domain boundary segments, φ_j is the magnetic scalar potential given by the j-th domain boundary segment w_j. The magnetostatic energy is given as

$$E_{st} = \frac{1}{2} \sum_{k=1}^{N_b} \int_{w_k} \varphi \sigma_k dS = \frac{1}{2} \sum_{k=1}^{N_b} \sum_{j=1}^{N_b} \int_{w_k} \varphi_j \sigma_k dS \qquad (8)$$

The magnetic scalar potential φ_j is given as follows. A rotated coordinate system (s, t, z) is used as illustrated in Fig. 2, where the s-axis is parallel to the j-th domain boundary segment. The end points of the domain boundary segment are denoted by (s_{j1}, t_j) and (s_{j2}, t_j). The potential φ_j is given as

$$\varphi_j(s,t,z) = \frac{\sigma_j}{4\pi\mu_0} \int_{s_{j1}}^{s_{j2}} \int_0^d \frac{dz_j ds_j}{\sqrt{(s-s_j)^2 + (t-t_j)^2 + (z-z_j)^2}}$$

$$= \frac{\sigma_j}{4\pi\mu_0} \{ f(s-s_{j1}, t-t_j, z-d) - f(s-s_{j1}, t-t_j, z) $$
$$- f(s-s_{j2}, t-t_j, z-d) + f(s-s_{j2}, t-t_j, z) \} \qquad (9)$$

where function $f(x, y, z)$ is given by

$$f(x,y,z) = y \tan^{-1} \frac{xz}{y\sqrt{x^2+y^2+z^2}} + z \ln(\sqrt{x^2+y^2+z^2} - x)$$
$$+ x \ln(\sqrt{x^2+y^2+z^2} - z) \qquad (10)$$

The integration of φ_j on the k-th domain boundary segment in Eq. (8) is performed analytically along the z-direction and numerically along the other direction.

The sequential quadratic programming (SQP) [6] method is used to determine the positions of endpoints of domain walls and the direction of normalized magnetization vectors that give a local minimum of total magnetic energy. To avoid the direct computation of Hessian matrix, the BFGS (Broyden-Fletcher-Goldfarb-Shanno) scheme [6] is used in the SQP, which is an efficient quasi-Newton scheme. Geometric constraints are imposed for the endpoints of domain walls.
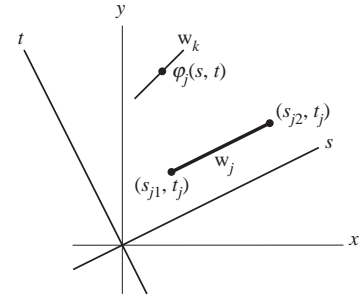

Fig. 2. Coordinate system for magnetic scalar potential.

3. Improvement of domain structure model

As is shown later, the DSM described above sometimes fails to represent magnetization processes of magnetic materials. Accordingly, this study modifies the DSM as below. The original and modified DSMs are called "SDSM" (simple DSM) and "MDSM" hereafter.

3.1. Vanishing factor for domain disappearance

When the position of a magnetic domain wall coincides with a material boundary because of domain wall movement, the domain between them disappears as is shown in Fig. 3. The disappearance of domain implies the vanishing of the domain wall. However, the domain wall energy of Eq. (5) may remain if the energy minimization procedure fails to decrease

θ_{wj} to zero. To avoid this residual domain wall energy, the domain wall energy E_{wj} is multiplied by a vanishing factor v_j defined as

$$v_j = v(\alpha_{j1})v(\alpha_{j2}) \ , \quad v(\alpha) = \begin{cases} 1 & (\beta \le \alpha) \\ 1-(1-\dfrac{\alpha}{\beta})^2 & (0 \le \alpha < \beta) \end{cases}$$

$$(11)$$

where $\alpha_{ji} = S_{ji} / l_{ji}$ ($i = 1, 2$) are defined for the two adjacent domains to the j-th domain wall; l_{ji} is the perimeter of domain ji, and S_{ji} is its area; β is a constant to give the domain size at which the vanishing factor begins to work. An index of domain width is given by α_{ji} even for a complexly shaped domain.
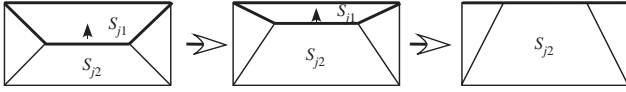
Fig. 3. Disappearance of magnetic domain.

3.2. Two-step SQP

The SQP sometimes fails to minimize E because the quadratic approximation using the BFGS formula does not always work well for the mixed variables of domain-wall endpoint positions and magnetization angles under geometric constraints of endpoint positions.

On the other hand, in an actual magnetization process, the domain wall movement usually occurs before the magnetization rotation proceeds.

Accordingly, to improve the energy minimization process, this study divides the SQP procedure into two steps; the domain wall positions are firstly optimized and the magnetization directions are optimized secondly.

4. Comparison with micromagnetic simulation

Four types of magnetic thin films with uniaxial anisotropy below are examined:

(IA) 8μm (easy axis direction) × 4μm × 20nm,
(IB) 16μm (easy axis direction) × 8μm × 20nm,
(IIA) 2μm × 1μm (easy axis direction) × 20nm, and
(IIB) 8μm × 4μm (easy axis direction) × 20nm.

A back-and-forth magnetic field is applied with an amplitude of 8×10^4 A/m along the direction of the longest edge. $M = 1.0$ T and $A = 1.3 \times 10^{-11}$ J/m are used for the simulation whereas K_1 is set at 5.0×10^2 J/m³ for films (IA) and (IB), and at 5.0×10^4 J/m³ for (IIA) and (IIB).

Micromagnetic simulations are executed by solving the LLG equation using unit cells of 15.625nm × 15.625nm × 10nm for films (IA), (IIA) and (IIB), and a unit cell of 31.25nm × 31.25nm × 10nm for film (IB).
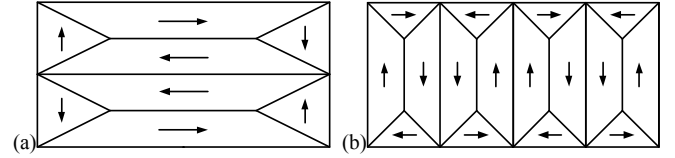

Fig. 4. Assumed domain structures; (a) for films (IA) and (IB), and (b) for films (IIA) and (IIB).
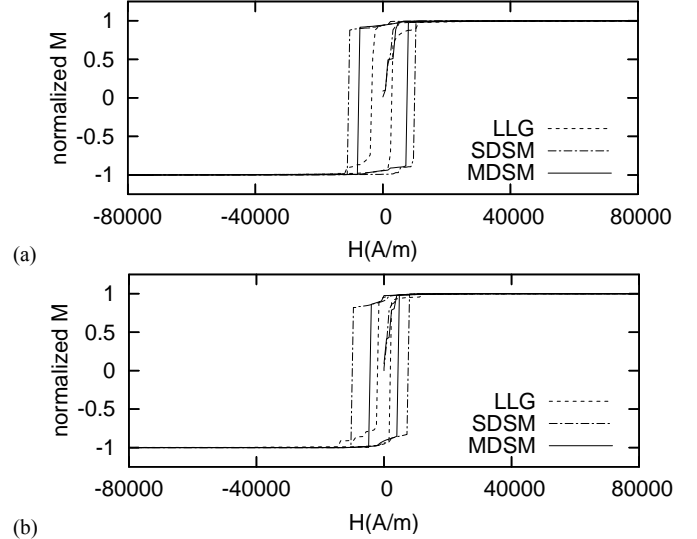

Fig. 5. Averaged MH loops along the applied field direction; (a) film (IA) and (b) film (IB).

4.1. Simulation with applied field along easy axis

The SDSM and MDSM are examined for films (IA) and (IB) where the domain structure shown by Fig. 4(a) is assumed.

Fig. 5 shows averaged MH loops along the easy axis direction that are given by the DSMs and the micromagnetic simulation. The comparison shows that the MDSM yields more accurate MH loops than the SDSM. Fig. 6 illustrates the domain structures of film (IB) obtained by the MDSM. Fig. 7 depicts those given by the micromagnetic simulation where brightness shows the perpendicular component of magnetization to the applied field direction. The domain structure obtained by the MDSM qualitatively agrees with that given by the micromagnetic simulation. Further improvement of the MDSM will be required to obtain quantitative agreement with the micromagnetic simulation.

A direct comparison of computational time is not easy between the micromagnetic simulation and the DSMs because the former was executed by a supercomputer and the latter were executed by a PC. The computational time for the DSM is not much affected by the analyzed material size if the same domain structure is assumed. In contrast, the computation time for the micromagnetic simulation rapidly increases with an increase in the number of cells. For example, it is estimated that the micromagnetic simulation for film (IB) requires about 200 times more computation time than the DSM.
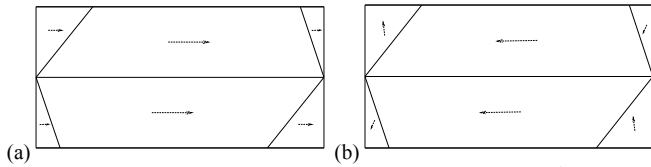
Fig. 6. Domain structures obtained by MDSM; (a) $H_{ap} = 8\times10^4$ A/m and (b) $H_{ap} = 1.6\times10^3$ A/m (when H_{ap} is increasing).

Fig. 9. Domain structures obtained by MDSM; (a) $H_{ap} = 0$ A/m and (b) $H_{ap} = -4\times10^4$ A/m.

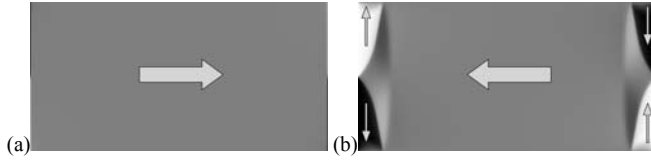Fig. 7. Magnetic domains given by the micromagnetic simulation; (a) $H_{ap} = 8\times10^4$ A/m and (b) $H_{ap} = 1.6\times10^3$ A/m (when H_{ap} is increasing).
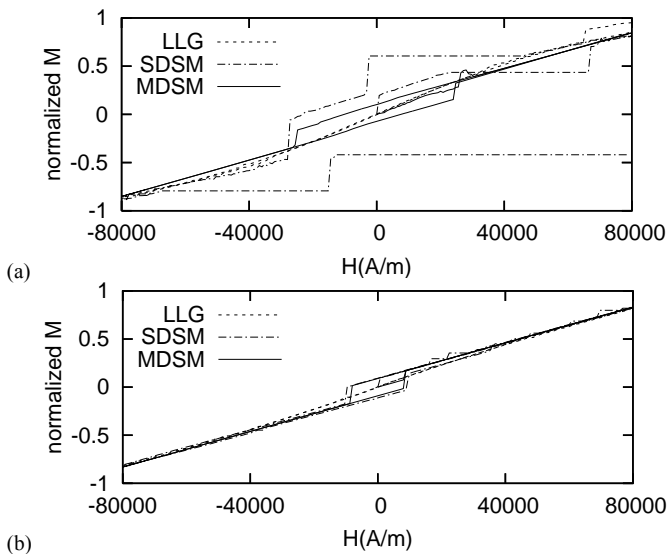

Fig. 10. Magnetic domains given by the micromagnetic simulation; (a) $H_{ap} = 0$ A/m and (b) $H_{ap} = -4\times10^4$ A/m.

5. Concluding remarks

This paper modifies a domain structure model (DSM) to improve its representation capability for domain behavior. A comparison with micromagnetic simulation shows that the modification effectively improves the representation accuracy of the magnetization process. The DSM is more efficient than the micromagnetic simulation when the analyzed material size becomes large.

Acknowledgments

Fig. 8. Averaged MH loops along the applied field direction; (a) film (IIA) and (b) film (IIB).

References

[1] H. Kronmüller, M. Fähnle, Micromagnetism and the Microstructure of Ferromagnetic Solids, Cambridge University Press, 2003.
[2] N. Smith, IEEE Trans. Magn. 24 (1988) 2380.
[3] C. Saka, K. Siiki, K. Shinagawa, J. Appl. Phys. 68 (1990) 263.
[4] M. Enokizono, T. Todaka, Y. Midou, IEEE Trans. Magn. 32 (1996) 1172.
[5] T. Matsuo, H. Sugino, M. Shimasaki, Papers Technical Meeting IEE Japan MAG-05-108 (2005).
[6] J.F. Bonnans, J.C. Gilbert, C. Lemaréchal, C.A. Sagastizábal, Numerical Optimization: Theoretical and Practical Aspects, 2nd Ed., Springer-Verlag, Berlin, 2006.

4.2. Simulation with applied field perpendicular to easy axis

The DSMs are examined for films (IIA) and (IIB) where the domain structure shown by Fig. 4(b) is assumed.

Fig. 8 shows averaged MH loops along the applied-field direction. Fig. 8(a) shows that the SDSM fails to represent magnetization reversal for film (IIA) whereas the MDSM gives accurate MH curve. Fig. 9 illustrates the domain structures of film (IIB) obtained by the MDSM whereas Fig. 10 depicts those yielded by the micromagnetic simulation. The former qualitatively agrees with the latter. Figs. 9 and 10 show that triangle domains assumed in Fig. 4(b) disappear, where the SDSM yields excess domain wall energ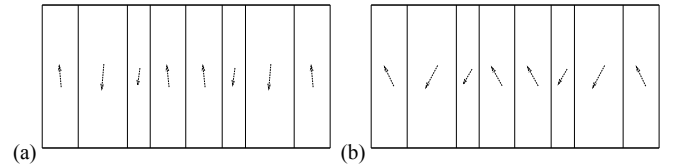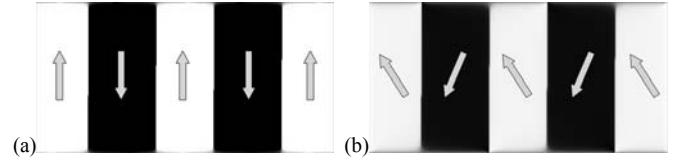y without the vanishing factor.